Accurate Modeling of Laser-Plasma Accelerators with Particle-In-Cell Codes

Estelle Michel[*], B. A. Shadwick[†,**], C. B. Schroeder[†], C. G. R. Geddes[†], E. Esarey[†,*], W. P. Leemans[†,*], H. Ruhl[‡] and T. Cowan[*]

[*]*Nevada Terawatt Facility, University of Nevada, Reno, Nevada 89507*
[†]*Lawrence Berkeley National Laboratory, Berkeley, California 94720*
[**]*Institute for Advanced Physics, Conifer, CO 80433*
[‡]*Ruhr University Bochum, 44780 Bochum, Germany*

Abstract. Particle-In-Cell (PIC) codes are often used to study systems where the details of phase-space are important; for example, self trapping or optical injection in laser-plasma accelerators. Here we investigate the numerical heating and macro-particle trajectory errors in 2D PIC simulations of laser-plasma accelerators. The effects of grid resolution and laser polarization on the momentum spread and on subsequent spurious trapping in a plasma wave is studied. It is shown that when the laser is polarized in the plane of the simulation, which mimics the 3D behavior, the macro-particles are subject to trajectory errors resulting in a high momentum spread. The phase-space error associated with this momentum spread results in unphysical trapping. Smoother particle shapes are considered to reduce the interpolation errors. With these schemes, the macro-particle trajectories are more accurately modeled and unphysical momentum spread is reduced.

Keywords: Particle-In-Cell, numerical heating

INTRODUCTION

Particle-in-cell (PIC) codes [1, 2] are a widely used tool to study laser plasma interactions, and in particular, have been used extensively to model laser-plasma based accelerator experiments [3], where a large amplitude wave is driven by a short laser pulse, and background electrons can become trapped in the plasma wake and be accelerated to high energies [4].

In a particle-grid approach such as PIC, finite-sized, charged "macro-particles" interact with electromagnetic fields defined on a grid. The unavoidable discretization of the physical model and the necessarily small number of macro-particles relative to the number of physical electrons both give rise to unphysical heating [1, 2]. In addition, since the macro-particle positions are not restricted to mesh points, some form of interpolation is necessary to evaluate the force, resulting in trajectory errors. These numerical heating mechanisms will alter phase space and can mimic physical processes leading to incorrect interpretation of computational results. This heating will be of particular importance when attempting to model detailed kinetic effects, such as trapping of the background electrons or generation of dark current in a plasma-based accelerator.

In the following we study the effect of the unphysical heating in PIC codes in the particular case of a weakly non-linear plasma wave driven by a short laser pulse. The normalized laser intensity is $a_0 = 1.15$ where $a_0^2 \approx 7.32\ 10^{-19}\,(\lambda_0[\mu m])^2\, I_0[W/cm^2]$ for a linear polarized laser pulse of wavelength λ_0 and intensity I_0. The laser propagates

in a parabolic plasma channel matched to its spot size, r_0 [3]. On axis the density of the plasma is such that $\omega_0/\omega_p = 10$ where $\omega_p = k_p c = (4\pi n_0 e^2/m_e)^{1/2}$ is the plasma frequency at the density n_0, and $\omega_0 = 2\pi c/\lambda_0$. The 2D simulation box is 65 μm long and 153 μm wide. The macro-particles are loaded uniformly and cold (no initial momentum), using 4 macro particles per cell. For the simulations, we use a modified version of Plasma Simulation Code (PSC) [5], which implements the standard PIC algorithm [1] and uses a charge-conserving current-deposition scheme [6].

For this illustrative case we expect no self-trapping in the wake because the plasma is loaded cold, and the laser intensity is sufficiently low such that the longitudinal plasma wakefield $E_z < E_0$, where $E_0 = m_e c^2 k_p/e$ is the cold, one-dimensional nonrelativistic wavebreaking-field. For a cold plasma, the particle orbits are identical to the cold fluid orbits, and thus trapping can only occur in conjunction with a singularity in the plasma density. The cold fluid model [7] does not show singular plasma density for these parameters, which is a definitive indication that there should be no trapping in this example. Note that the evolution of the plasma temperature has previously been studied using a warm fluid model [8, 9], which predicts that an initially cold collisionless plasma remains cold in this regime; i.e., a delta function momentum distribution remains a delta function and is an exact solution of the Vlasov equation. Thus we expect that the PIC simulation with an initially cold plasma should converge to the cold fluid result. However, the PIC simulations show macro-particles trapped in the wake, as seen in Fig. 1. Note that at this resolution the longitudinal electric field is almost converged. For definiteness we consider trapped macro-particles with $p_z/m_e c > 1$, which is the peak momentum for untrapped particles in this case. The trapped charge depends on the resolution, number of macro-particles per cell used and on the laser polarization. The observed trapping is due to the numerical heating of the plasma; the associated increase of momentum spread leads to the trapping in the wake [10].

This case is near the trapping threshold and is thus quite sensitive to numerical heating. Such test cases are of interest since threshold behaviour is important, even when the trapping results from an instability such as Raman scattering, in determining quantities such as bunch size, emittance and energy spread.

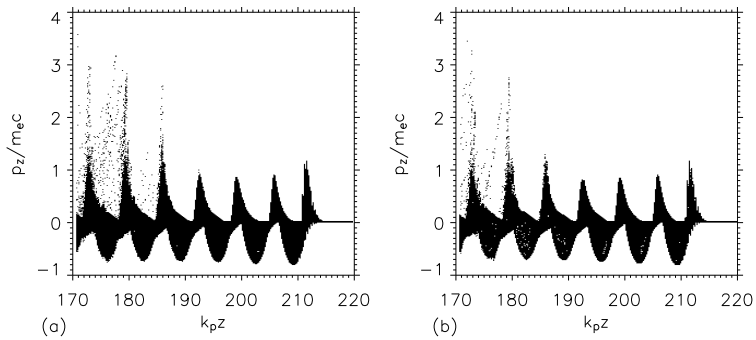

FIGURE 1. Longitudinal phase-space of the electrons at $\omega_p t \approx 218$, with the laser polarized (a) in the plane of the simulation, (b) out of the plane of the simulation. The resolution is $dx = \lambda_0/2.5 = r_0/32$ and $dz = \lambda_0/24$.

POLARIZATION DEPENDENCE

Shown in Fig. 2 are the macro-particle orbits. For the case of laser polarization out of the simulation plane [see Fig. 2(b)] the trajectories of the macro-particles correspond to a nearly laminar flow, which is the expected result for an initially cold plasma. However, when the laser is polarized in the plane of the simulation [see Fig. 2(a)] interpolation errors lead to significant perturbation of the macro-particle orbits near the end of the laser pulse, i.e., the macro-particles experience a field interpolation error owing to the under-resolved grid, leading to an error in the momentum advance in the fast ($\omega_0/\omega_p \gg 1$) laser oscillations.

The error introduced by the field interpolation at the macro particle position is estimated by introducing analytically prescribed fields, and looking at test particle orbits in the transverse plane, the laser being polarized in this same plane (i.e. the x direction). In Fig. 3(a) two test particles are initially loaded on axis (same transverse position) and in the same cell but separated longitudinally by $dz/2$, where dz is the grid size along the direction of laser propagation. After the laser pulse, the two particles have different final momenta, which gives rise to trajectory crossing seen in Fig. 2(a). Figures 3(b) and 3(c) show the effect of the different resolutions on the particle trajectory error. The main role is played by the longitudinal resolution which needs to well resolve the laser wavelength; a resolution of at least $dz \lesssim \lambda_0/50$ is necessary to reduce the macro-particle

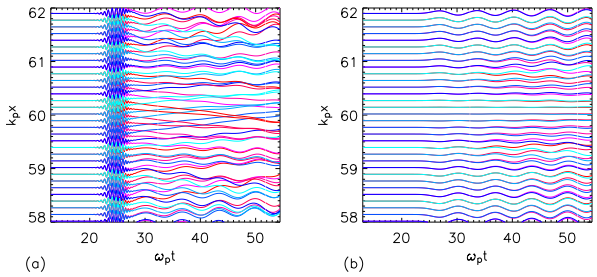

FIGURE 2. Macro-particle orbits at $\omega_p t \approx 55$, for transverse resolution $dx = \lambda_0/2.5$ and longitudinal resolution $dz = \lambda_0/24$. (a) The laser is polarized in the plane of the simulation. (b) The laser is polarized out of the plane of the simulation. Note that the laser is centered at $k_p x \approx 60$.

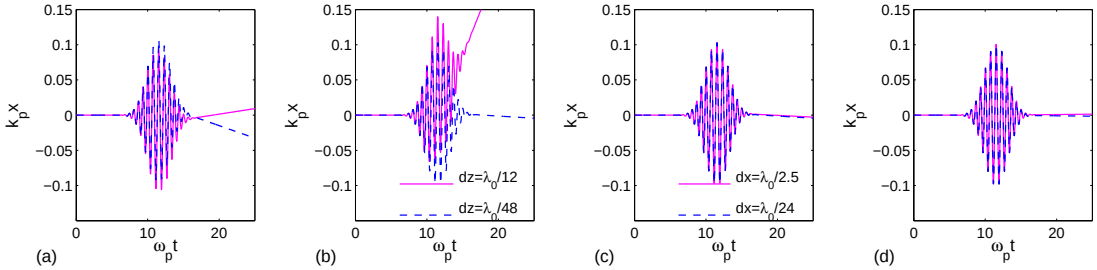

FIGURE 3. Orbit of two test particles initially on axis and in the same cell with: (a) $dx = dz = \lambda_0/24$ using linear interpolation, (b) $dx = \lambda_0/24$ and different longitudinal resolutions using linear interpolation, (c) $dz = \lambda_0/48$ and different transverse resolutions using linear interpolation, and (d) $dx = dz = \lambda_0/24$ using parabolic particle shape.

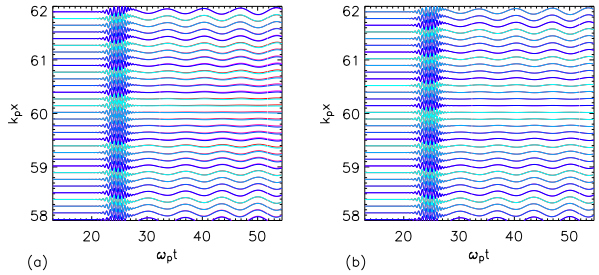

FIGURE 4. Macro-particle orbits at $\omega_p t \approx 55$, for transverse resolution $dx = \lambda_0/2.5$ and longitudinal resolution $dz = \lambda_0/24$, using (a) parabolic and (b) cubic particle shapes.

trajectory error to a negligible level.

Using smoother particle shapes significantly decreases the trajectory error. PIC codes typically use linear weighting, also called Cloud-In-Cell [11]; higher order interpolation schemes (smoother particle shapes) are obtained by convolving the square (Nearest-Grid-Point) weighting function with itself *m*-times (see Ref. [1] Sect. 8-8, Ref. [2] Sect. 5-3-4 and Ref. [12]), the scheme remaining charge conserving. The macro-particle orbits with the quadratic and cubic particle shapes are shown in Figs. 4(a) and Fig. 4(b), respectively, the laser being polarized in the simulation plane. In these cases the macro-particles follow a laminar flow as expected. Indeed, Fig. 3(d) shows that the trajectory error inside the laser pulse, with the quadratic particle shape, is suppressed. In Fig. 4(a) we still notice macro-particle orbit separation owing to the numerical heating, which is absent from Fig. 4(b).

Shown in Fig. 5 are macro-particle trajectories computed using linear interpolation with the addition of smoothing using a (1,2,1) filter with compensator (See Ref. [1] Appendix C and Ref. [13]) on the current densities. As expected, we see a reduction of the heating when the laser is polarized out of the plane of the simulation, but significant trajectory errors remain. This suggests that smoother particle shapes are more efficient than smoothing for obtaining accurate trajectories.

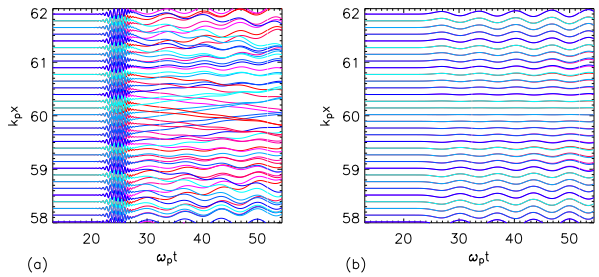

FIGURE 5. Macro-particle orbits at $\omega_p t \approx 55$, for transverse resolution $dx = \lambda_0/2.5$ and longitudinal resolution $dz = \lambda_0/24$, using the linear interpolation scheme and current smoothing with compensator: (a) in the plane polarization and (b) out of the plane polarization.

PLASMA TEMPERATURE

We can distinguish two heating mechanisms [Fig. 7(c)]: scattering [14], with a continuous slow growth rate due to the finite number of macro-particles, which depends mainly on the number of macro-particles per cell and on the particle shape; and grid heating [15], with a fast growth rate and saturates when $\lambda_D \sim dz$ in 1D, where $\lambda_D = \left(T/4\pi ne^2\right)^{1/2}$ is the Debye length, and dz the grid size.

Figure 6(a) shows the transverse RMS momentum spread, $\sigma^2_{u_x} = \langle (u_x - \langle u_x \rangle)^2 \rangle$ (where $u_x = p_x/m_e c$ is the normalized momentum), on axis for the in and out of the plane polarization cases, using the linear interpolation scheme. When the laser is polarized in the plane of the simulation, it triggers a larger momentum spread, due to the macro-particle trajectory errors, and the grid heating saturation value is reached sooner. Figures 6(b) and 6(c) show the resolution dependence, when the laser is polarized out of the plane. The grid heating is reduced when the transverse resolution [Fig. 6(b)], i.e., the largest grid size is reduced. Figure 7 shows the effect of using smoother particle shapes. The discrepancy between in and out of the plane polarization vanishes [Fig. 7(a)], since the momentum spread introduced by the trajectory errors is suppressed; the temperature is much lower after the laser pulse when using smoother particle shapes [Fig. 7(b)]. The cubic interpolation does not reduce the scattering inside the laser pulse compare to the quadratic scheme, but the scattering growth rate is lower after the laser and the grid

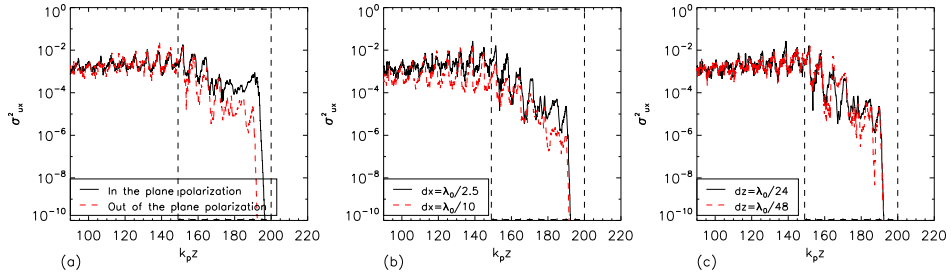

FIGURE 6. Transverse momentum spread for linear particle shape: (a) $dx = \lambda_0/2.5$ and $dz = \lambda_0/24$ in and out of the plane polarizations, (b) $dz = \lambda_0/24$, changing transverse resolution, and (c) $dx = \lambda_0/2.5$, changing longitudinal resolution. The dashed box indicates the size of the simulation box used in Fig. 1.

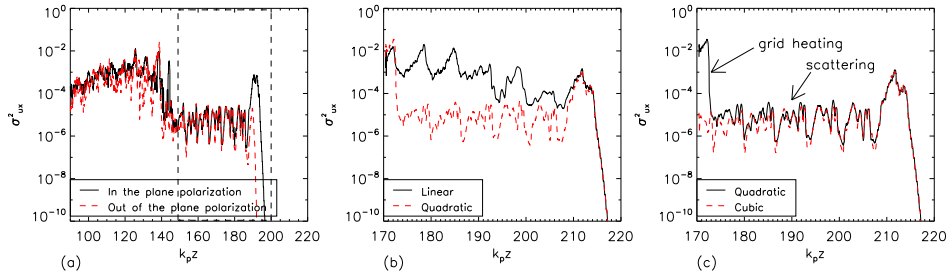

FIGURE 7. Transverse momentum spread for $dx = \lambda_0/2.5$ and $dz = \lambda_0/24$: (a) quadratic particle shape, in and out of the plane polarizations; (b) in the plane polarization, linear and quadratic, and (c) in the plane polarization quadratic and cubic particle shapes.

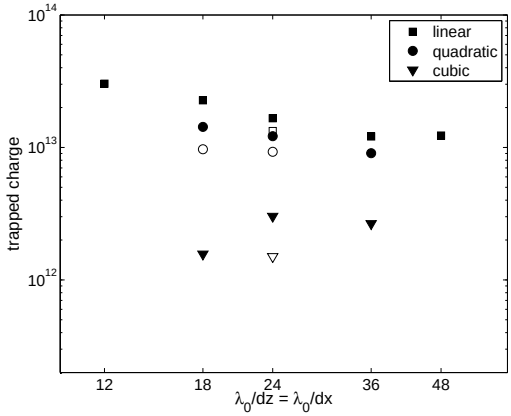

FIGURE 8. Amount of charge trapped ($p_z/m_e c > 1$) versus resolution, with $dx = dz$, for different interpolation algorithms: (square) linear interpolation, (circle) quadratic interpolation, and (triangle) cubic interpolation. Full and empty points are for, respectively, 4 and 16 macro-particles per cell. The laser is polarized in the plane of the simulation.

heating is delayed [Fig. 7(c)]. Increasing the number of macro-particles per cell also decreases the momentum spread due to scattering, for quadratic and cubic particle shapes; the effect is not present for linear interpolation as the temperature is dominated by the trajectory errors, when the laser is polarized in the plane of the simulation.

The results are summarized in Fig. 8 where the number of trapped macro-particles in the 2D simulations has been normalized in order to give a charge per meter. With linear interpolation, the amount of trapping saturates when the grid becomes sufficiently small (dx, $dz \lesssim \lambda_0/36$), i.e., reducing the grid is not sufficient to reduce the heating. One has to use more macro-particles per cell or use smoother particle shapes because, at this resolution, the temperature at which grid-heating saturates does not lead to significant trapping and heating due to macro-particle scattering (which is independent on grid size) dominates the phase-space errors. Indeed, the cubic particle shape reduces significantly the amount of trapped charge. Moreover, it is less computationally expensive to use smoother particle shapes than using more macro-particles.[1] The case studied here is close to the self-trapping threshold and, hence, convergence is slow; although using the cubic particle shapes reduces the trapping to the last plasma wave bucket in the simulation window. This means than one may need to use rather high resolution to reach convergences in some cases, especially when one wants to determine the threshold for trapping (e.g. when studying optical injection or dark current generation).

---

[1] Quadratic particle shapes increase the computing time by approximately 25% and there is less than a factor of two between the computational expense of the linear and the cubic interpolation schemes.

CONCLUSION

We have demonstrated that misleading results, e.g. spurious trapping, can be obtained with PIC codes if the resolution used is not sufficiently high, particularly when one studies phenomena close to the self-trapping threshold. We have shown a strong dependence of unphysical heating on the laser polarization with respect to the plane of the 2D simulation. In particular, the motion of the macro-particles in the laser pulse, when polarized in the simulation plane, leads to trajectory errors, unless the longitudinal resolution is extremely high (i.e., higher than the resolutions typically used to model laser-plasma accelerators). Moreover, the grid heating imposes high resolution in all dimensions. We have shown that using smoother particle shapes results in a more accurate description of the particle motion and reduces the unphysical heating of the plasma.

ACKNOWLEDGMENTS

This work was supported by the University of Nevada, Reno, grant DE-FC52-01NV14050, by the Director, Office of Science, Office of High Energy Physics, of the U.S. Department of Energy under Contract No. DE-AC02-05CH11231, and by a Scientific Discovery through Advanced Computing project, "Advanced Computing for 21st Century Accelerator Science and Technology" and INCITE grant, which are supported by the US DOE/SC Office of High Energy Physics and the Office of Advanced Scientific Computing Research. This research used resources of the National Energy Research Scientific Computing Center.

REFERENCES

1. C. Birdsall, and A. Langdon, *Plasma Physics via Computer Simulation*, Institute of Physics Publishing, Bristol, 1991.
2. R. Hockney, and J. Eastwood, *Computer Simulation using Particles*, Taylor & Francis Group, New York, 1988.
3. E. Esarey, P. Sprangle, J. Krall, and A. Ting, *IEEE Trans. on Plasma Sci.* **24**, 252–288 (1996).
4. S. P. D. Mangles *et al*., Nature **431**, 535 (2004); C. G. R. Geddes *et al*., *ibid.* **431** 538 (2004); J. Faure *et al*., *ibid.* **431**, 541 (2004).
5. H. Ruhl, *Collective Super-Intense Laser-Plasma Interaction*, Habilitationsschrift, Technische Universität Darmstadt (2000).
6. T. Z. Esirkepov, *Comput. Phys. Commun.* **135**, 144 (2001).
7. B. A. Shadwick, G. M. Tarkenton, E. H. Esarey, and W. P. Leemans, *IEEE Trans. Plasma Sci*. **30**, 38 (2002).
8. B. A. Shadwick, G. M. Tarkenton, and E. Esarey, *Physical Review Letters* **93**, 175002 (2004).
9. B. A. Shadwick, G. M. Tarkenton, E. Esarey, and C. B. Schroeder, *Phys. Plasmas* **12**, 056710 (2005).
10. C. B. Schroeder, E. Esarey, B. A. Shadwick, and W. P. Leemans, *Phys. Plasmas* **13**, 033103 (2006).
11. C. K. Birdsall, and D. Fuss, *J. Comput. Phys.* **3**, 494 (1969).
12. H. Abe, N. Sakairi, R. Itatani, and H. Okuda, *J. Comput. Phys.* **63**, 247 (1986).
13. W. B. Mori (2006), (private communication).
14. R. W. Hockney, *J. Comput. Phys.* **8**, 19 (1971).
15. A. B. Langdon, *J. Comput. Phys.* **6**, 247 (1970).